Journal of Physical Science, Vol. 34(1), 1–20, 2023

Formaldehyde Cross-Linked Chitosan as Silver-Nanoparticles Stabiliser For Cr(VI) Ion Sensor Application

Sulistyani,[1*] Isana Supiah Yosephine Louise,[1] Susila Kristianingrum,[1] Annisa Fillaeli,[1] Atiya Fiki Rahma Mumtazah,[1] Bian Itsna Ashfa Al Ashfiya[2] and Wipsar Sunu Brams Dwandaru[2]

[1]Department of Chemistry Education, Faculty of Mathematics and Natural Sciences, Universitas Negeri Yogyakarta, Jl. Colombo, No. 1, Karangmalang, Yogyakarta 55281, Indonesia
[2]Department of Physics Education, Faculty of Mathematics and Natural Sciences, Universitas Negeri Yogyakarta, Jl. Colombo, No. 1, Karangmalang, Yogyakarta 55281, Indonesia

Correspondence E-mail: sulistyani@uny.ac.id; wipsarian@uny.ac.id

Published online: 28 April 2023

To cite this article: Sulistyani et al. (2023). Formaldehyde cross-linked chitosan as silver-nanoparticles stabiliser for Cr(VI) ion sensor application. *J. Phys. Sci.*, 34(1), 1–20. https://doi.org/10.21315/jps2023.34.1.1

To link to this article: https://doi.org/10.21315/jps2023.34.1.1

ABSTRACT: *We report for the first time a technique in the detection of chromium(VI) [Cr(VI)] ions using ultraviolet-visible (UV-Vis) spectrophotometer that involves silver nanoparticles (AgNPs) capped with formaldehyde-chitosan as the sensor. Here, chitosan cross-linked with formaldehyde produced an extra stability from the aspect of signal stability of the sensor. This study aimed to synthesise and characterise formaldehyde-chitosan stabilised AgNPs (formaldehyde-chitosan@AgNPs) and apply them as Cr(VI) ion sensors. The stability and linearity of the signal of the formaldehyde-chitosan@AgNPs were compared with the signal of AgNPs according to their ability as Cr(VI) ion sensors based on the UV-Vis spectroscopy. The AgNPs were synthesised by the chemical reduction method using 1% sodium citrate (10:1). Furthermore, 3.3% chitosan was added, which had been cross-linked with 2.5% formaldehyde in a ratio of 1:1 (v:v). The characterisation results showed that the synthesised materials have a peak absorption at a wavelength of 416 nm and have functional groups of -OH and -C=O as the characteristics of chitosan and formaldehyde. The formaldehyde-chitosan@AgNPs had square or rectangular structures with a size distribution of less than 1000 nm. The formaldehyde-chitosan@AgNPs produced a more stable signal and had better linearity than AgNPs at a wavelength of 490 nm. Moreover, formaldehyde-chitosan@AgNPs had a precision value of 0.15% and a linearity level of 0.9914 in the concentration range of 1 ppm–100 ppm,*

with limit of detection (LOD) and limit of quantisation (LOQ) values of 0.329 ppm and 0.751 ppm, respectively.

Keyword: silver nanoparticles, formaldehyde, chitosan, Cr(VI) ion sensor

1. INTRODUCTION

Industrial development nowadays has improved the quality of human life. However, this rapid development can also have negative impacts. Solid and liquid wastes have adverse effects on the surrounding environment; such as the presence of chromium metal (Cr) in leather tanning waste, electroplating, and 'batik' colouring industry.[1] The Cr(VI) ions have undesirable properties, i.e., they are difficult to decompose, unstable and more toxic than Cr(III) ions.[2] The release of the metallic Cr into the environment causes pollution that can potentially harm living things. Hence, the prevention of the metallic Cr being released into the environment may be conducted by the detection of metal ions.

Heavy metal detection usually uses inductive coupled plasma (ICP) and atomic absorption spectroscopy (AAS) instruments.[3–6] However, these instruments measure the number of total metal atoms, whereas analytical techniques based on their specific ions are often required. Ultraviolet-visible (UV-Vis) spectrophotometer is a standard tool used for metal analysis by its species. However, ion analysis with this technique generally requires a complexing agent, e.g., Cr(III) ion added with Ethylenediaminetetraacetic acid (EDTA) and Cr(VI) ion added with diphenylcarbazide (DPC) ligands.[7] Compound analysis using UV-Vis spectrophotometer is in great demand because it is relatively easy and fast, and the instruments are widely available in the laboratory. In the last decade, several UV-Vis spectrophotometric detection techniques have been developed by involving nanoparticles as sensors.[8–11]

Nanoparticles are granules or solid particles ranging in size from 10 nm to 1000 nm.[12] Gold and silver are metal nanoparticles that are widely used as sensors, especially for detecting the presence of heavy metals because of their optical properties, such as surface plasmon resonance (SPR) and their ability to aggregate. Silver nanoparticles (AgNPs) have better optical properties than gold nanoparticles (AuNPs). AgNPs have several advantages, e.g., they have higher molar absorption coefficient at the same amount.[13] This makes AgNPs visible if they are characterised using the UV-Vis spectrophotometer. Economically, silver is relatively inexpensive and easy to produce. However, AgNPs are chemically unstable, that is, they easily agglomerate. Hence, efforts are needed to maintain the particles at the nano scale and prevent agglomeration.

A sensor is a device that receives an external stimulus and then responds to that stimulus as an electrical signal. The stimulus can be physical, chemical or biological signals, which are then converted into electrical signals in the form of current, voltage or charge.[14] SPR is a resonance phenomenon between light at a specific wavelength and electrons on a metal surface producing electron oscillations on the metal surface. At a particular frequency, the light resonates, producing a localised electric field called localised SPR (LSPR).[15] This phenomenon encourages the application of AgNPs as a sensor. The ability of nanoparticles to act as a metal ion sensor is an application of the metal nanoparticles' SPR absorption.[16] The addition of a capping agent to metal nanoparticles causes interactions between the capping agent and nanoparticles, which results in changes and shifts in the SPR.[17]

The excellent optical properties of AgNPs make them potential to be developed as sensors, in this case, colorimetric device. A factor that needs to be considered in colorimetry is the selection of organic components as ligands to modify the nanoparticles. The organic molecule can give a specific response to the analyte, such that there is a change in the colour and UV-Vis spectrum due to the aggregation of nanoparticles.[18] In its application as a colorimetric sensor, AgNPs can be modified with organic compounds used as ligands or capping agents and can affect the SPR. Ligand-modified AgNPs have been applied to analyse the presence of small molecules, such as proteins and toxic metals.[13] Gelatine, polyvinyl alcohol (PVA) and chitosan are some of the substances that can be used as ligands in modifying nanoparticles.[19]

Several things affect the SPR value, including nanoparticle size, shape, capping agent, state of aggregation and environment. The smallest particle size usually results in high surface energy for the nanoparticles.[20] Factors that can affect the particle size in the nanoparticle synthesis include solution temperature, salt concentration, reducing agent and reaction time.[21] The LSPR of AgNPs is very sensitive to local refractive index changes induced by bonding of the analyte at or near the surface of the nanoparticles. The narrow plasmon bandwidth in AgNPs allows for more accurate measurements of the LSPR shift.[22]

AgNPs are very easy to agglomerate due to the low level of stability. Therefore, it is necessary to add a stabiliser to AgNPs, one of which is chitosan. The addition of chitosan in nanoparticles can provide sufficient steric barrier to stabilise colloids and increase the function of nanoparticles as sensors.[10,23,24] However, chitosan is soluble in acidic conditions, so chitosan is at risk of being released from the surface of AgNPs when used as a modifying agent, especially in acidic conditions. Hence, chitosan needs to be cross-linked to increase its stability. The types of aldehydes and anhydrous are often used as cross-linking agents because they are relatively inexpensive and easy to obtain such as, formaldehyde, dialdehyde, glutaraldehyde, and anhydrous acetate.[22,25–27]

In this study, the AgNPs stabilised by chitosan are cross-linked with formaldehyde to form formaldehyde-chitosan@AgNPs. Moreover, the performance of the nanocomposites is tested as a Cr(VI) ion sensor using the UV-Vis spectrophotometer. To the knowledge of the authors, this study is the first to provide a technique in the detection of Cr(VI) ions using UV-Vis spectrophotometer that involves AgNPs capped with formaldehyde-chitosan as the sensor. Here, chitosan cross-linked with formaldehyde produces an extra stability from the aspect of signal stability of the sensor. From this study, it is hoped that the Cr(VI) ions detection using a UV-Vis spectrophotometer becomes more simple, sensitive and reliable.

2. EXPERIMENTAL

2.1 Tools and Materials

The tools and materials used in this study are given as follows. The tools used were ultraviolet-visible (UV-Vis) Shimadzu UV-2450 spectrophotometer, Fourier transform infrared (FTIR) Nicolet Avatar 360 IR, particle size analyser (PSA) Microtac Nanotrac Wave II, scanning electron microscope (SEM) JEOL JSM-6510LA, hot plate, magnetic stirrer, analytical balance and standard glassware. The materials used were $AgNO_3$, HCl, $K_2Cr_2O_7$, sodium citrate, formaldehyde, chitosan and aqua demineralised (DM). The chemicals were purchased from Merck, Germany with analytical-reagent grade and no further purification.

2.2 Synthesis of AgNPs

$AgNO_3$ solution with a concentration of 1.0×10^{-3} M as much as 50 ml was heated until it boiled. Then 5 ml of 1% sodium citrate was added to the solution, drop by drop. During the heating process at a temperature of 60°C, stirring was carried out using a magnetic stirrer to make the solution homogeneous. The heating process was continued until the solution's colour became pale yellow. The temperature was kept constant at 60°C throughout the heating process. After that, the heating process was stopped, but the solution was still stirred until its temperature has reached room temperature.

2.3 Synthesis of Formaldehyde-Chitosan@AgNPs

A concentration of 37% of chitosan was dissolved in 1% hydrochloric acid to a final concentration of 3.3%. Moreover, formaldehyde in the form of gel with a concentration of 2.5% was added with a ratio of 1:1 (v:v) to the chitosan. Then, the formaldehyde cross-linked chitosan was added to the AgNP solution obtained above and stirred until homogeneous.

2.4 Characterisation of Formaldehyde-Chitosan@AgNPs

The synthesised formaldehyde-chitosan@AgNPs were characterised using UV-Vis spectrophotometer, FTIR, PSA and SEM. The characterisation by UV-Vis spectrophotometer was to ensure the formation of AgNPs based on the peak absorption in the range of 400 nm. The PSA profile analysis was conducted to determine the particle size distribution of the synthesised formaldehyde-chitosan@AgNPs. The FTIR analysis was conducted to identify the functional groups of chitosan and formaldehyde. The FTIR characterisation was only conducted upon the formaldehyde-chitosan@AgNPs because the functional groups of chitosan and formaldehyde were different, i.e., the former were dominated by amine and hydroxyl, whereas the latter was dominated by carbonyl. The SEM was used to determine the surface morphology of the formaldehyde-chitosan@AgNPs.

2.5 Formaldehyde-Chitosan@AgNPs as Cr(VI) Ion Sensor

The ability of formaldehyde-chitosan@AgNPs as Cr(VI) ion sensor was compared with the ability of AgNPs for the same purpose via the UV-Vis spectrophotometer. The formaldehyde-chitosan@AgNPs and AgNPs interacted with Cr(VI) ions at various concentrations. The concentration of Cr(VI) ion varied was in the range of 1 ppm to 100 ppm.

As many as 13 volumetric flasks of 25 ml were prepared. Each volumetric flask was filled with 1.67 ml of AgNPs. Then, 100 ppm stock solution of Cr(VI) were added into each volumetric flask to make the concentration of the Cr(VI) ions to become 1 ppm, 3 ppm, 5 ppm 7 ppm, 10 ppm, 15 ppm, 20 ppm, 25 ppm, 30 ppm, 40 ppm, 50 ppm, 75 ppm, and 100 ppm, then marked with distilled water. Furthermore, the solution was homogenised. After 5 min of the mixing process, the absorption measurements were carried out in the wavelength range of 300 nm –700 nm. The above steps and mixing time duration were repeated for 1.92 g of formaldehyde-chitosan@AgNPs.

2.6 Identification of Analytical Performance

Identifying analytical performance includes precision, linearity, the limit of detection (LOD) and the limit of quantisation (LOQ). Therefore, the coefficient of variance percentage (%CV) and the standard deviation (SD) were used, i.e.,

$$\%\mathrm{CV} = (\mathrm{SD}/\mathrm{y}) \times 100\%, \tag{1}$$

and

$$SD = \left(\sum(y - \bar{y})/(n-1)\right)^{1/2}, \quad (2)$$

where y is the signal height, $\bar{y}$ is the average signal height and n is the amount of the data.

The linear regression equation was determined by making a curve of the relationship between the concentration of the analyte solution and the absorption value. In general, the regression equation obtained was y = bx + a, where y = A (absorption value), x = C (concentration of the analyte solution), a is the intercept and b is the slope. The LOD was calculated based on a standard signal involving a signal-to-noise ratio of 3 to 1, while the LOQ is determined by a signal-to-noise ratio of three times the LOD value.[28]

3. RESULTS AND DISCUSSION

AgNPs are obtained by reducing $AgNO_3$ solution using sodium citrate. The AgNPs formed are marked by the colour change of the solution from pale yellow to yellow. As time progresses, the colour of the solution becomes brownish. The colour change of the solution to brownish occurs after stirring the AgNPs for 1 h. The colour change was due to the excitation of surface plasmon vibrations of the AgNPs.[29] The colour change of the AgNP solution is also affected by the concentration of the solution. The greater the concentration, the faster the colour changes. The ability of sodium citrate as a reducing agent is to reduce silver ions (Ag^+) to Ag^0 according to the reaction equation (3). Furthermore, AgNPs are stabilised with chitosan-formaldehyde. Physically, the formaldehyde-chitosan@ AgNPs appear more viscous, forming a gel as shown in Figure 1.

$$4Ag^+ + C_6H_5O_7Na_3 + 2H_2O \rightarrow 4Ag^0 + C_6H_5O_7H_3 + 3Na^+ + H^+ + O_2 \quad (3)$$

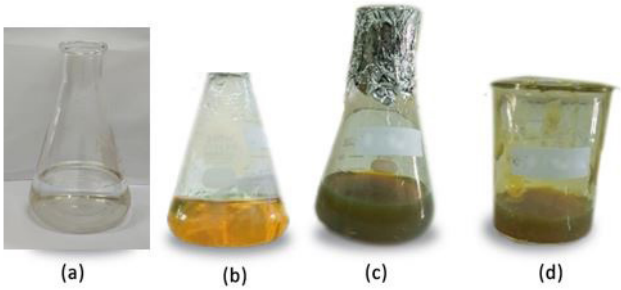

Figure 1: (a) The initial colour of the $AgNO_3$ and sodium citrate mixture, (b) the AgNP solution formed after heating, (c) the AgNP solution after stirring for 1 h and (d) the formaldehyde/chitosan/AgNPs.

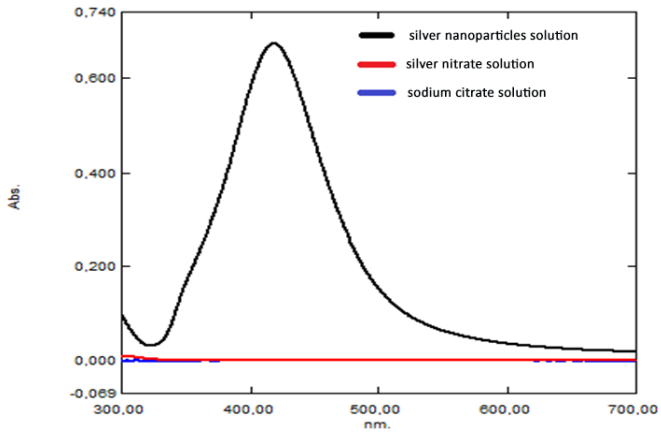

Figure 2: Absorption spectra of the sample solutions.

The formation of AgNPs is strengthened by the measurement results of the UV-Vis spectrum. AgNPs have a maximum absorption peak in the wavelength range of 400 nm–450 nm. This is in accordance with previous experiments that the maximum absorption of AgNPs is at a wavelength of about 400 nm.[10,16,30] The absorption value obtained indicates the number of AgNPs formed. The higher the absorption value, the greater the number of AgNPs produced. The absorption peak of the synthesised AgNPs is shown in Figure 2. Based on the UV-Vis absorption spectrum results in Figure 2, the $AgNO_3$ and sodium citrate solution before being mixed does not have a peak. However, after the two solutions were mixed, a maximum peak appeared at a wavelength of 417.50 nm, which indicates the presence of a new component formed after mixing. The presence of an absorption peak indicates that the AgNPs have been successfully synthesised.

The synthesised AgNPs have advantages such as being able to be applied to colorimetric tests. However, the AgNPs also have a weakness that is easy to agglomerate. Modifications on the AgNPs can use ligands that can prevent AgNPs' aggregation. Chitosan is a polysaccharide biopolymer ligand resulting from chitin deacetylation, which is known to have the ability to stabilise AgNPs so that the size of AgNPs does not increase.[24] Increasing the stability of chitosan can be done by adding cross-linking agents such as formaldehyde because chitosan is soluble in acidic conditions.[26] The modification of the AgNPs in this study is carried out by cross-linking chitosan and formaldehyde with a ratio of 1:1. The cross-linked chitosan with formaldehyde is added to the AgNP solution during the cooling process and stirred until homogeneous.

The formaldehyde-chitosan@AgNPs are further characterised using the UV-Vis spectrophotometer. The comparison of the absorption peaks between AgNPs, formaldehyde-chitosan@AgNPs and chitosan@AgNPs is shown in Figure 3. Based on Figure 3, it is shown that the absorption peaks of AgNPs, chitosan@AgNPs and formaldehyde-chitosan@AgNPs occur at the same wavelength, i.e., no chemical shift occurs. Similarly, the absorption of the SPR region at a wavelength of 490 nm between the three spectra shows almost the same signal. Overall, the presence of chitosan-formaldehyde covering the surface of the AgNPs does not significantly affect the energy of the electrons of the AgNPs. This is possible because the interaction between chitosan-formaldehyde and AgNPs is more physical in the form of van der Waals forces.

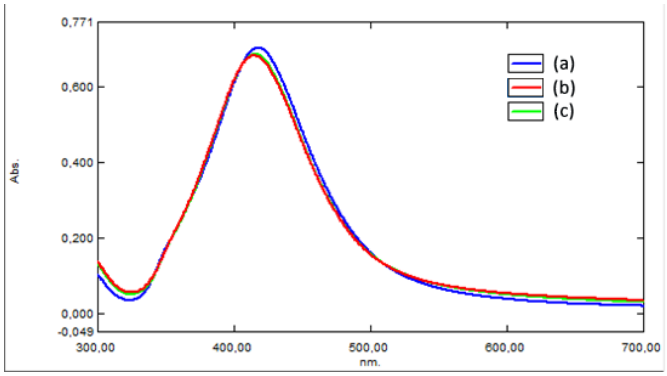

Figure 3: (a) Absorption spectra comparison of AgNPs, (b) chitosan/AgNPs and (c) formaldehyde/chitosan/AgNPs.

Furthermore, formaldehyde-chitosan@AgNPs were tested for stability to prove that the formaldehyde cross-linked chitosan can maintain the stability of AgNPs. The stability of formaldehyde-chitosan@AgNPs is measured within 1 h at its

absorption peak. The stability of formaldehyde-chitosan@AgNPs can be seen in Figure 4. The addition of chitosan-formaldehyde to AgNPs increases the stability of AgNPs. The absorption profile of the absorption peak of the AgNPs without adding chitosan-formaldehyde decreases rapidly after just 5 min, while the absorption profile of the formaldehyde-chitosan@AgNPs is relatively constant. Possibly, the AgNPs without chitosan-formaldehyde undergoes aggregation. Thus, adding the chitosan-formaldehyde succeeded in maintaining the stability of the AgNPs. Aggregation of metal nanoparticles tends to occur quickly because of the strong electron cloud between metal atoms. However, in the presence of chitosan-formaldehyde, the distances between the AgNP atoms are relatively further apart, thereby weakening the strength of the electron cloud.

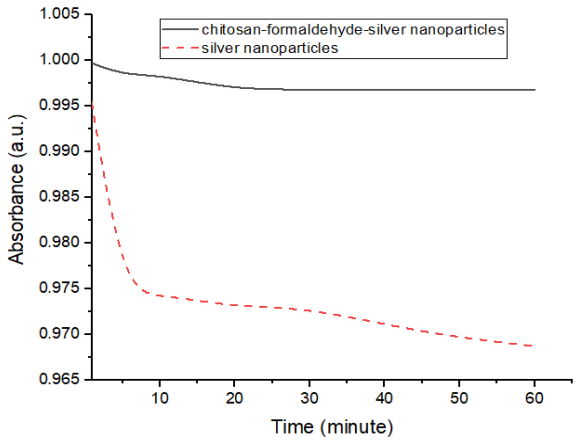

Figure 4: Comparison of the stability of AgNPs and formaldehyde/chitosan/AgNPs at the absorption peak.

The success of chitosan-formaldehyde binding to AgNPs can be observed in the FTIR spectrum. Chitosan has amine ($-NH_2$) and hydroxyl (-OH) groups that can interact with transition metal cations to stabilise AgNPs. Formaldehyde has a -CH group and a C=O group to bind to the chitosan. Figure 5 shows a wide absorption at the wave number of 3,445.31 cm^{-1}, indicating the -OH group. There is also a C=O group at a wave number of 1,636.76 cm^{-1} with a sharp absorption intensity. The absence of absorption that shows the NH group at wave numbers between 3,500 cm^{-1}–3100 cm^{-1} is possible because the absorption of the hydroxyl group (-OH) overlaps with the amine group ($-NH_2$). The presence of amine and carbonyl groups in chitosan causes chitosan to either donate or accept electrons. This drives the electrostatic force between chitosan-formaldehyde and AgNPs and other metal atoms.

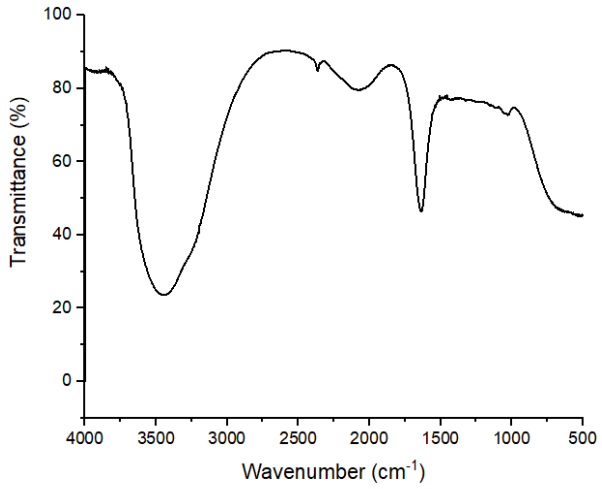

Figure 5: FTIR spectrum of formaldehyde/chitosan/AgNPs.

The particle size distribution of the AgNPs is observed by the PSA, which may be observed in Figure 6. Based on Figure 6, formaldehyde-chitosan@AgNPs have sizes below 1,000 nm, i.e., 244.8 nm, as much as 17% and also above 1,000 nm, i.e., 1,970 nm, as much as 50%. This indicates that the synthesis of the AgNP from $AgNO_3$ is not yet fully achieved. On the other hand, most of the synthesised nanoparticles are possibly undergoing aggregation, so that their size tends to be large.

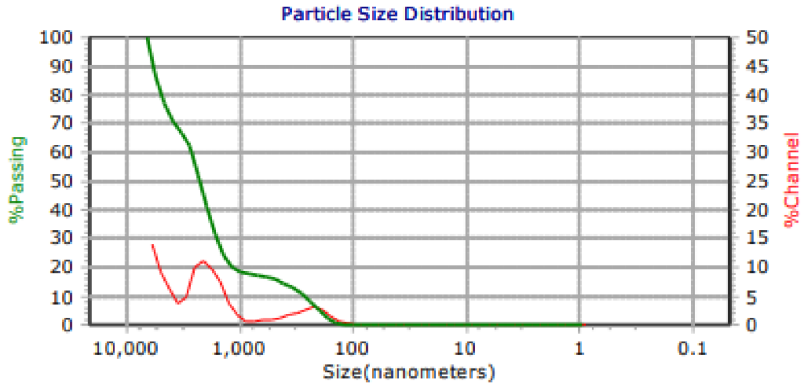

Figure 6: PSA spectrum of formaldehyde/chitosan/AgNPs.

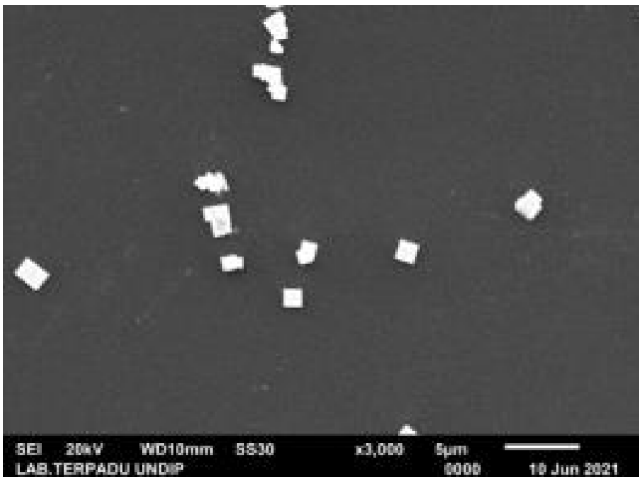

Figure 7: Morphology of formaldehyde/chitosan/AgNPs with 3,000x magnification using SEM.

Figure 7 shows the surface morphology of the formaldehyde-chitosan@AgNPs after being characterised using the SEM-EDX instrument at a certain magnification. The surface morphology of the sample with a magnification of 3,000× shows that the sample is square or rectangular. The large particle size is due to agglomeration, so the particle size increases. Drying using an oven allows forming less stable chitosan/AgNPs. In addition, another factor that can cause particle agglomeration is the high concentration of chitosan used to form the gel. This is because the high concentration of reducing and stabilising agents provides a larger growth space for the AgNPs.[19] The SEM-EDX test was also used to determine the elemental content in the sample. The graph of elemental content in the formaldehyde-chitosan@AgNPs sample can be seen in Figure 8.

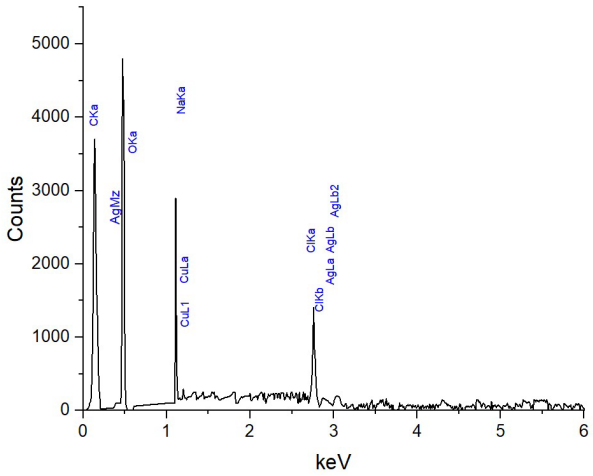

Figure 8: EDX result for formaldehyde/chitosan/AgNPs.

Based on the EDX results in Figure 8, the carbon (C) element has the largest mass percentage, which is 79.82%. Chitosan and formaldehyde contain C elements as the dominant constituent of formaldehyde-chitosan@AgNPs, while O elements have a percentage of 3.9%. The Na element derived from sodium citrate has the second largest amount with a percentage of 10.41%. The chlorine (Cl) element with a percentage of 4.12% came from the solvent of chitosan. Meanwhile, the presence of copper (Cu) elements is possibly due to the existence of impurities that come from the materials used in the synthesis process. Furthermore, the Ag element derived from the $AgNO_3$ precursor solution contained in the formaldehyde-chitosan@AgNPs has a small amount of 1.00%.

Observation of AgNPs using UV-Vis spectrophotometer can be seen by the presence of the LSPR. LSPR is a strong interaction between metal nanoparticles and the electromagnetic field of light, causing oscillations in the delivery of electrons on the nanoparticle's surface to the cationic region.[13] SPR arises because of the influence of the chemical environment that contains positive and negative charges. Based on the absorption spectrum in Figure 3, AgNPs and formaldehyde-chitosan@AgNPs form the SPR signal at a wavelength of 490 nm. This could be because the chains of chitosan and formaldehyde are quite short, so they do not affect the SPR.

The emergence of SPR can be used as a biosensor or chemical sensor. SPR is an optical sensor that utilises surface plasmon waves to observe the interaction of metal surfaces, either gold or silver, with dielectric materials.[31] Testing of AgNPs

in detecting Cr(VI) ion is carried out by reacting AgNPs with Cr(VI) ion with various concentrations. The characterisation of the formaldehyde-chitosan@ AgNPs in detecting metals is carried out by measuring the absorption spectrum of UV-Vis in the wavelength range of 300 nm–700 nm. Testing the AgNPs as a sensor of Cr(VI) ions is identified by interacting AgNPs with Cr(VI) ions at different concentrations. The absorption spectrum of AgNPs-Cr(VI) ion is carried out in the wavelength range of 300 nm–700 nm.

The absorption profiles between AgNPs and formaldehyde-chitosan@AgNPs with Cr(VI) ions are shown in Figure 9. Based on the spectra of both samples, it can be observed that the interaction with Cr(VI) ions causes a peak absorption shift, i.e., a hypochromic shift to 350 nm. This is possible because the Cr(VI) ion interacts strongly in a dipole-dipole interaction with the electrons on the surface of the AgNPs. Hence, it requires higher excitation energy. In addition, the SPR signal at a wavelength of 490 nm of the spectrum is larger as the concentration of the Cr(VI) ions increases. If both samples are compared, the SPR absorption of the formaldehyde-chitosan@AgNPs sample is greater than the AgNPs, as observed in Table 1. This indicates that the presence of chitosan-formaldehyde on the surface of the AgNPs affects their chemical environment.

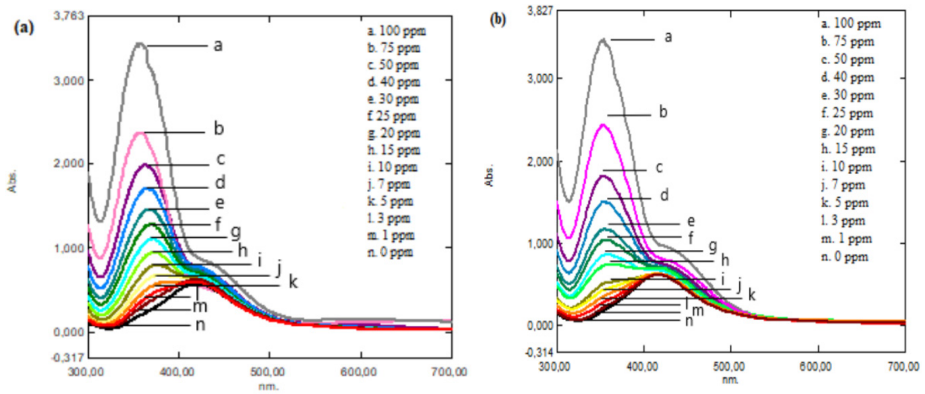

(a) (b)

Figure 9: (a) Absorption spectra of AgNPs interacted with Cr(VI) ion and (b) formaldehyde/ chitosan/AgNPs interacted with Cr(VI) ion at different concentrations.

Table 1: The absorption value of AgNPs and formaldehyde/chitosan/AgNPs interacted with Cr(VI) ions in the SPR region (490 nm).

Concentration (ppm)	Absorption	
	AgNPs	formaldehyde-chitosan@AgNPs
0	0.180	0.195
1	0.194	0.193
3	0.180	0.193
5	0.184	0.207
7	0.191	0.215
10	0.193	0.203
15	0.191	0.216
20	0.199	0.221
25	0.209	0.230
30	0.218	0.242
40	0.233	0.252
50	0.241	0.258
75	0.206	0.293
100	0.308	0.343

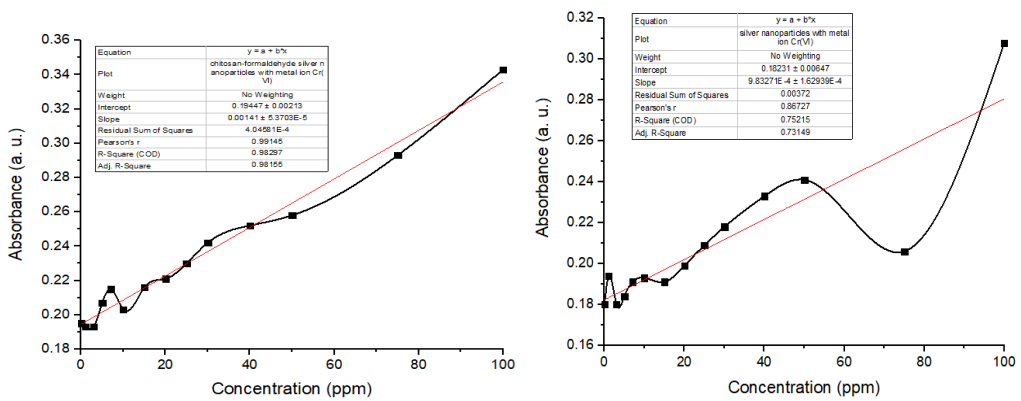

(a) (b)

Figure 10: (a) Linearity test of AgNPs and (b) formaldehyde/chitosan/AgNPs with metal ion Cr(VI) at 490 nm.

In this study, a comparison of the analytical performance tests between AgNPs and formaldehyde-chitosan@AgNPs has been carried out, especially for linearity, to determine which sample acts better as a Cr(VI) ion sensor on a UV-Vis spectrophotometer. The linearity test is carried out by making an absorption calibration curve, i.e., the correlation between the concentration of Cr(VI) ion and the absorbance in the SPR region (490 nm). Based on the results of the analysis, the linearity value (R^2) of AgNPs is 0.7521 with the regression equation of $y = 0.001x + 0.1823$ [Figure 10(a)], while the linearity value (R^2) of formaldehyde-chitosan@AgNPs is 0.983 with the regression equation of $y = 0.0014x + 0.145$ [Figure 10(b)] in a concentration range of 1 ppm–100 ppm. Based on these regression equations, it can be stated that the formaldehyde-chitosan@AgNPs particles as a Cr(VI) ion sensor on UV-Vis spectrophotometer have better linearity than AgNPs over a wide concentration range. Thus, it can be said that the formaldehyde-chitosan@AgNPs are recommended as Cr(VI) ion sensors. Furthermore, the lower value of the R^2 for the AgNPs compared to the formaldehyde-chitosan@AgNPs may be caused by the AgNPs degradation as they interact with the Cr(VI) ions as the ion concentration is increased. On the other hand, the formaldehyde/chitosan acts as stabiliser for AgNPs in the formaldehyde-chitosan@AgNPs, hence their interaction with Cr(VI) ions do not degrade the AgNPs. This shows that the formaldehyde cross-linked chitosan manages to stabilise the AgNPs especially in their interaction with the Cr(VI) ions.

Furthermore, the analytical performance of formaldehyde-chitosan@AgNPs is determined based on the value of precision, LOD and LOQ. Precision states repeatability, the closeness between one data and other data obtained in a similar fashion. Precision values are usually expressed in %CV. In this study, the %CV value of the formaldehyde-chitosan@AgNPs is 0.15% (see Table 2). The precision of the data is considered good if it gives a 95% confidence level, which means that the error is small (%CV not more than 5%). Thus, the signal precision in the study is considered good. The detection limit is the lowest concentration of analyte in the sample, which still shows the instrument's absorption without meeting the criteria of accuracy and precision. The LOQ is the smallest amount of analyte in the sample that can still be measured accurately and precisely by the instrument.[32] The LOD and LOQ values of this study are 0.329 ppm and 0.751 ppm, respectively. Based on the analysis of the precision values, sensitivity levels, linearity tests, and detection limits, it can be stated that the formaldehyde-chitosan@AgNPs as a sensor of Cr(VI) ions have good analytical performance.

Table 2: Identification of the signal precision.

y	$\bar{y}$	$y - y$	$\left(y - y\right)^2$
0.628		0.001	0.000001
0.627		0	0
0.627		0	0
0.626	0.627	–0.001	0.000001
0.626		–0.001	0.000001
0.626		–0.001	0.000001
0.626		–0.001	0.000001
			Σ = 0.000005
		SD = 0.000913	
		%CV = 0.15%	

Table 3: Comparison of different optical approaches for Cr(VI) ions detection.

Method	**Material**	**Detection Limit**	**Linear Range**	**Ref.**
Fluorescence	Si QDs	0.65 μmol L^{-1}	1.25–40 μmol L^{-1}	33
	C-Dots	0.03 μg ml^{-1}	0.10–12 μg ml^{-1}	34
Colorimetric	AuNPs	280 nmol L^{-1}	0.5–50.0 μmol L^{-1}	35
	Ag core–Au shell nanoparticles	10 nmol L^{-1}	0.02–8 μmol L^{-1}	36
	AgNPs	1 nmol L^{-1}	10^{-3}–10^{-9} mol L^{-1}	37
	Cu@AuNPs	0.21 nmol L^{-1}	0.4–1000 nmol L^{-1}	38
Fibre Bragg grating	Sol–gel monoliths	10 ppb	–	39
	Hydrogel	10 ppb	–	40

Finally, a comparison of different optical approaches for Cr(VI) ions detection from previous studies can be seen in Table 3. According to Table 3, the detection of Cr(VI) ions is generally carried out on the ppb or mol L^{-1} unit, while the range of the Cr(VI) ions detection in this study is in the ppm or mmol L^{-1} unit. However, the need for Cr(VI) detection does not always require analytical methods at low concentrations (below 1 ppm), but sometimes Cr(VI) ions detection at higher concentrations are needed in some cases so as not to do many dilutions. Excessive dilution reduces the accuracy and reliability of measurement results.

This study seeks to determine the performance of AgNP capped with chitosan-formaldehyde on the ppm scale, which turns out to have a wide linear range up to 100 ppm with a very good linearity level, even better than AgNP capped with chitosan without cross-linker. This broad linearity value indirectly indicates the interesting possibility of using formaldehyde-chitosan@AgNPs as a Cr(VI) ion sensor at a lower scale, i.e., μg ml^{-1} to ng ml^{-1}.

4. CONCLUSION

Formaldehyde-chitosan@AgNPs nanocomposites are successfully synthesised with characteristics having an absorption peak at a wavelength of 416 nm, square or rectangular-shaped structures, and a size distribution of 244.8 nm by 17%. According to the FTIR spectrum, the chitosan-formaldehyde is successfully linked to AgNPs, which shows hydroxyl (-OH) and carbonyl (-C=O) functional groups. For the application as a Cr(VI) ion sensor, the formaldehyde-chitosan@AgNPs produce a more stable signal and have better linearity than AgNPs at a wavelength of 490 nm. Furthermore, the formaldehyde-chitosan@AgNPs have a precision value of 0.15%, a linearity level of 0.9914 in the concentration range of 1 ppm–100 ppm, with LOD and LOQ values of 0.329 ppm and 0.751 ppm, respectively.

5. ACKNOWLEDGEMENTS

The authors would like to thank the Mathematics and Natural Sciences Faculty, Universitas Negeri Yogyakarta for funding this research through the DIPA UNY with the contract No. B/20/UN34.13/PT.01.03/2021.

6. AUTHORS' NOTE

The authors declare that there is no conflict of interest regarding the publication of this manuscript. Moreover, the authors confirm that the manuscript is free of plagiarism.

7. REFERENCES

1. Ackerley, D. F. et al. (2004). Chromate-reducing properties of soluble flavoproteins from *Pseudomonas putida* and *Escherichia coli*. *Appl. Environ. Microbiol.*, 70(2), 873–882. https://doi.org/10.1128/AEM.70.2.873-882.2004
2. Oliveira, H. (2012). Chromium as an environmental pollutant: Insights on induced plant toxicity. *J. Bot.*, 2012, 1–8. https://doi.org/10.1155/2012/375843

3. Bagherian, G. et al. (2019). Determination of copper(II) by flame atomic absorption spectrometry after its perconcentration by a highly selective and environmentally friendly dispersive liquid–liquid microextraction technique. *J. Anal. Sci. Technol.*, 10(3). https://doi.org/10.1186/s40543-019-0164-6
4. Didukh-Shadrina, S. L. et al. (2019). Determination of metals in natural waters by inductively coupled plasma optical emission spectroscopy after preconcentration on silica sequentially coated with layers of polyhexamethylene guanidinium and sulphonated nitrosonaphthols. *Int. J. Anal. Chem.*, 2019, 1–13. https://doi.org/10.1155/2019/1467631
5. Manousi, N. & Zachariadis, G. A. (2020). Development and application of an ICP-AES method for the determination of nutrient and toxic elements in savory snack products after autoclave dissolution. *Separations*, 7(4), 66. https://doi.org/10.3390/separations7040066
6. Shaltout, A. A. & Ibrahim, M. A. (2007). Detection limit enhancement of Cd, Ni, Pb and Zn determined by flame atomic absorption spectroscopy. *Can. J. Anal. Sci. Spectrosc.*, 52(5), 276–286. https://www.researchgate.net/publication/236761762
7. Soares, R. et al. (2009). Simultaneous speciation of chromium by spectrophotometry and multicomponent analysis. *Chem. Spec. Bioavailab.*, 21(3), 153–160. https://doi.org/10.3184/095422909X466095
8. Juliasih, N. et al. (2017). Application of ZnO Nanoparticle as sulphide gas sensor using UV/VIS/NIR-Spectrophotometer. *J. Phys. Conf. Ser.*, 824, 012020. https://doi.org/10.1088/1742-6596/824/1/012020
9. Liu, G. et al. (2018). Visual and colorimetric sensing of metsulfuron-methyl by exploiting hydrogen bond-induced anti-aggregation of gold nanoparticles in the presence of melamine. *Sensors*, 18(5), 1595. https://doi.org/10.3390/s18051595
10. Sugunan, A. et al. (2005). Heavy-metal ion sensors using chitosan-capped gold nanoparticles. *Sci. Technol. Adv. Mater.*, 6(3–4), 335–340. https://doi.org/10.1016/j.stam.2005.03.007
11. Willner, M. R. & Vikesland, P. J. (2018). Nanomaterial enabled sensors for environmental contaminants. *J. Nanobiotechnology*, 16(1), 95. https://doi.org/10.1186/s12951-018-0419-1
12. Mohanraj, U. J. & Chen, Y. (2006). Nanoparticles - A review. *Trop. J. Pharm. Res*., 5(1), 561–573. https://doi.org/10.4314/tjpr.v5i1.14634
13. Caro C. et al. (2010). Sensing and imaging applications. In D. P. Perez (Ed.). *Silver Nanoparticole*. United Kingdom: InTech. https://doi.org/10.5772/8513
14. Patel, B. C. et al. (2020). *Advances in modern sensors: Physics, design, simulation and applications*. IOP Publishing.
15. Novotny, L. & Hecht, B. (2006). *Principles of nano-optics*. United Kingdom: Cambridge University Press. 378–414. https://doi.org/10.1017/CBO9780511794193
16. Tashkhourian, J. & Sheydaei, O. (2017). Chitosan capped silver nanoparticles as colorimetric sensor for the determination of iron(III). *Anal. Bioanal. Chem. Res.*, 4(2), 249–260. https://doi.org/10.22036/abcr.2017.69942.1127

17. Luo, Y. et al. (2010). Preparation, characterization and evaluation of selenite-loaded chitosan/TPP nanoparticles with or without zein coating. *Carbohydr. Polym.*, 82(3), 942–951. https://doi.org/10.1016/j.carbpol.2010.06.029
18. Xiong, D. & Li, H. (2008). Colorimetric detection of pesticides based on calixarene modified silver nanoparticles in water. *Nanotechnology*, 19(46), 465502. https://doi.org/10.1088/0957-4484/19/46/465502
19. Gusrizal, G. et al. (2017). Synthesis of silver nanoparticles by reduction of silver ion with m-hydroxybenzoic acid. *Asian J. Chem.*, 29(7), 1417–1422. https://doi.org/10.14233/ajchem.2017.2043
20. Oldenburg, S. J. (2011). *Silver nanoparticles properties and applications.* USA: Sigma Aldrich. Retrieved 10 December 2020, https://www.sigmaaldrich.com/ID/en/technical-documents/technical-article/materials-science-and-engineering/biosensors-and-imaging/silver-nanomaterials-properties
21. Sileikaite, A. et al. (2006). Analysis of silver nanoparticles produced by chemical reduction of silver salt solution. *J. Mater. Sci.*, 12(4), 287–291. https://matsc.ktu.lt/index.php/MatSc/article/view/26461
22. Lee, S. H. et al. (2007). Effect of the concentration of sodium acetate (SA) on crosslinking of chitosan fiber by epichlorohydrin (ECH) in a wet spinning system. *Carbohydr. Polym.*, 70(1), 53–60. https://doi.org/10.1016/j.carbpol.2007.03.002
23. Haryani, K. et al. (2011). Pembuatan khitosan dari kulit udang untuk mengadsorbsi logam krom (Cr^{6+}) dan tembaga (Cu). *Reaktor*, 11(2), 86. https://doi.org/10.14710/reaktor.11.2.86-90
24. Twu, Y. K. et al. (2008). Preparation of silver nanoparticles using chitosan suspension. *Powder Technol.*, 185(3), 251–257. https://doi.org/10.1016/j.powtec.2007.10.025
25. Kildeeva, N. R. et al. (2009). About mechanism of chitosan cross-linking with glutaraldehyde. *Russ. J. Bioorganic Chem.*, 35(3), 360–369. https://doi.org/10.1134/S106816200903011X
26. Singh, A. et al. (2006). External stimuli response on a novel chitosan hydrogel crosslinked with formaldehyde. *Bull. Mater. Sci.*, 29(3), 233–238. https://doi.org/10.1007/BF02706490
27. Wegrzynowska-Drzymalska, K. et al. (2020). Crosslinking of chitosan with dialdehyde chitosan as a new approach for biomedical applications. *Materials*, 13(15), 3413. https://doi.org/10.3390/ma13153413
28. Ogunbanwo, B. F. et al. (2015). Method validation and uncertainty report for the determination aflatoxins in melon seeds. *IAJMR*, 1(1), 73–80. https://www.researchgate.net/publication/275967544
29. Shankar, S. S. et al. (2004). Rapid synthesis of Au, Ag, and bimetallic Au core-Ag shell nanoparticles using Neem (Azadirachta indica) leaf broth. *J. Colloid Interface Sci.*, 275(2), 496–502. https://doi.org/10.1016/j.jcis.2004.03.003
30. Devaraj, P. et al. (2013). Synthesis and characterization of silver nanoparticles using cannonball leaves and their cytotoxic activity against MCF-7 cell line. *J. Nanotechnol.*, 2013, 1–5. https://doi.org/10.1155/2013/598328
31. Rhodes, C. et al. (2006). Surface plasmon resonance in conducting metal oxides. *J. Appl. Phys.* 100(5), 054905. https://doi.org/10.1063/1.2222070

32. Torowati & Galuh, B. S. (2014). Penentuan nilai limit deteksi dan kuantisasi alat titrasi potensiometer untuk analisis uranium. *Jurnal Batan*. 13, 9–15. https://jurnal.batan.go.id/index.php/pin/article/view/1371/1302
33. Phan, L. M. T. et al. (2018). Synthesis of fluorescent silicon quantum dots for ultra-rapid and selective sensing of Cr(VI) ion and biomonitoring of cancer cells. *Mater. Sci. Eng.* C. 93, 429–436. https://doi.org/10.1016/j.msec.2018.08.024
34. Vaz, R. et al. (2017). High luminescent carbon dots as an eco-friendly fluorescence sensor for Cr(VI) determination in water and soil samples. *J. Photochem. Photobiol. A: Chem*., 346, 502–511. https://doi.org/10.1016/j.jphotochem.2017.06.047
35. Guo, J., Huo, D., Yang, M., Hou, C., Li, J., Fa, H., Luo, H. & Yang, P. (2016). Colorimetric detection of Cr (VI) based on the leaching of gold nanoparticles using a paper-based sensor. *Talanta*, 161, 819–825. https://doi.org/10.1016/j.talanta.2016.09.032
36. Xin, J. et al. (2012). A rapid colorimetric detection method of trace Cr (VI) based on the redox etching of Ag(core)-Au(shell) nanoparticles at room temperature. *Talanta*, 101, 122–127. https://doi.org/10.1016/j.talanta.2012.09.009
37. Ravindran, A. et al. (2012). Selective colorimetric detection of nanomolar Cr(VI) in aqueous solutions using unmodified silver nanoparticles. *Sens. Actuators B Chem*., 166–167, 365–371. https://doi.org/10.1016/j.snb.2012.02.073
38. Li, J. et al. (2017). Core-shell Cu@Au nanoparticles as an optical probe for ultrasensitive detection of chromium(VI) via an etching effect. *Microchim. Acta*, 184, 3817–3823. https://doi.org/10.1007/s00604-017-2409-7
39. Zhu, L. et al. (2017). On–off–on fluorescent silicon nanoparticles for recognition of chromium(VI) and hydrogen sulfide based on the inner filter effect. *Sens. Actuators B Chem*. 238, 196–203. https://doi.org/10.1016/j.snb.2016.07.029
40. Kishore, P. V. N. et al. (2017). Detection of trace amounts of chromium(VI) using hydrogel coated Fiber Bragg grating. *Sens. Actuators B Chem.*, 243, 626–633. https://doi.org/10.1016/j.snb.2016.12.017